Hindawi
Journal of Electrical and Computer Engineering
Volume 2022, Article ID 2071454, 12 pages
https://doi.org/10.1155/2022/2071454

Research Article

Voltage Stability Assessments and Their Improvement Using Optimal Placed Static Synchronous Compensator (STATCOM)

Tebeje Tesfaw Wondie and Teshome Goa Tella

Department of Electrical and Computer Engineering (Power Engineering) at Addis Ababa Science and Technology University, Addis Ababa, Ethiopia

Correspondence should be addressed to Tebeje Tesfaw Wondie; gsr24512eeng@aastu.edu.et

Received 3 March 2022; Revised 6 July 2022; Accepted 28 July 2022; Published 23 August 2022

Academic Editor: Yang Li

In this paper, static voltage stability assessments and their improvement using analytical and optimization techniques with different loading scenarios are described. In this study, the 400 kV, 230 kV, and 132 kV Ethiopian electric power networks are modeled using Power System Analysis Toolbox (PSAT), and the load flow analysis is carried out using MATLAB source code. Then, different voltage stability indices, such as the user-defined advanced voltage stability index (AVSI), modified voltage stability index (MVSI), and fast voltage stability index (FVSI), are used to identify the voltage unstable buses. Besides this, particle swarm optimization (PSO) is also used to find the optimal size and placement of the Static Synchronous Compensator (STATCOM) for the most severe buses identified by voltage stability indices. The result presents three special arguments: whether the most severe buses that are ranked at the top based on the voltage stability indices are optimal buses for compensation placement or not, the voltage stability improvement, and power loss reduction with the introduction of STATCOM. Accordingly, it is observed that the weakest bus that is identified through the stability indices may not be the optimal placement of the compensation device. It is also indicated that, with the introduction of STATCOM to the optimal selected bus, the network power loss is reduced from 46.65 MW to 33.32 MW and its voltage magnitude in all buses is also improved. All bus voltages are within the IEEE standard acceptable limit.

1. Introduction

According to the definition of [1, 2], voltage stability is "the ability of a power system network to maintain steady state voltages in all buses before and after the network is being subjected to a disturbance from a given initial operating condition." Voltage stability is a subset of power system stability that deals with the bus voltage operational limitations before and after a disturbance. Voltage instability can result due to the loss of load in a given area or the tripping of transmission lines and malfunctioning of the circuit protective mechanisms, and it leads to cascading system outages. In the current scenario, the power utilization of the customers has been increasing drastically, which leads the power system to turn massively into a strained situation with decreased stability margins. Voltage stability problems are classified as small and large voltage stability problems based on the magnitude of disturbance and are also classified as long-term and short-term voltage stability based on the duration of the disturbances.

1.1. Overview of Ethiopian Electric Power Network. The Ministry of Water and Energy (MWE) of the Government of Ethiopia (GOE) manages, plans, directs, and monitors the total energy development in Ethiopia. The vertically integrated utility, Ethiopian Electric Power Corporation (EEPCo), was divided into two public enterprises in 2013 [3]: the Ethiopian Electric Power (EEP) Company, which is responsible for the generation and transmission sectors, and the Ethiopian Electric Utility (EEU), which is responsible for power distribution, sales, and transmission. The EEU also comprises the Ethiopian Energy Authority (EEA), which is responsible for setting effective regulations, directives, and

standards for the industry. According to the EEP data in May 2021GC, the total generated power installed capacity in Ethiopia is 4473.9 MW, of which 90.63% of the source of power is gained from hydro and the remaining 9.37% is gained from other sources.

In this paper, the Ethiopian electric power network is modeled using the Power System Analysis Tool (PSAT) software, as shown in Figure1. The power network model comprises 400 kV, 230 kV, and 132 kV overhead transmission lines with 17 generation stations. According to EEP data from May 2021, the system has 246 buses, 307 overhead transmission lines, and 17 generation stations in total. In Figure 1, the red, green, and blue colors show 132 Kv, 230 Kv, and 400 Kv transmission lines, respectively.

2. Related Work

The paper done by Okelola et al. [4] focused on the optimal location and size of STATCOM on the transmission line network using particle swarm optimization to enhance system voltage magnitude and reduce active power losses. The authors also used a single-objective function to compute particle swarm optimization.

Another paper done by Mahiraj et al. [5] explained the voltage stability using the line stability index (VSI_2) used to identify the weak transmission lines in the system. The paper also compares series and shunt compensators to improve the voltage profile. The authors tried to compare the Thyristor Control Series Capacitor (TCSC) and Static Synchronous Compensator (STATCOM) to enhance the voltage conditions. In conclusion, STATCOM has a greater capacity to improve the voltage profile than the series compensator.

The study done by Mezigebu et al. [6] described how STATCOM was included in the microgrid to enhance the voltage profile and decrease power loss. In the study, microgrid and STATCOM controllers connected to the grid are modeled using MATLAB/PSAT.

The STATCOM controllers are also carried out using Proportional Integral (PI) and Fuzzy Logic Controllers. The IEEE 30-bus system is also used to test the effectiveness of STATCOM with microgrid integrations to improve the voltage profile of the network. The study concludes that the STATCOM raises the distribution line capacity, improves the voltage profile, and reduces the power loss of the network. In the study, an integrated microgrid is connected at bus number 30 to improve the voltage profile. However, further investigation is required into the optimal placement of microgrids within the main system networks.

Another paper done by Bhongade et al. [7] focused on the Optimal Reactive Power Dispatch based on the result of the voltage collapse prediction index. The authors used STATCOM as a compensation device and the Voltage Collapse Prediction Index (VCPI) to determine the weakest bus on which the compensator device should be placed. Also, PSO and BAT algorithm techniques are used to find the optimal size of STATCOM. As a result, the authors tried to discuss the comparison of system active power loss with and without STATCOM connected to the weakest bus. The STATCOM is simply placed on the weakest bus, as determined by the voltage stability indices, as a result of the paper's findings. However, the weakest bus may not be the optimal placement of STATCOM, and it requires further investigation to verify the results obtained with voltage stability indices and optimization techniques.

2.1. Cases of Voltage Collapse Incident. The term "voltage collapse" refers to a series of events that occur as a result of voltage instability and result in a blackout or abnormally low voltages in a substantial portion of the power system. Voltage collapse could be a result of power system voltage instability. Voltage instability is a condition in which voltage drops to a very low level due to a succession of occurrences. Power system components such as lines, transformers, and/or generators tripping and consumption disturbances cause the voltage to collapse. Voltage collapse can also occur as a result of unexpected load changes, a lack of coordination between control parameters and the protection system, and frequency deviation. If there are not sufficient reactive power reserves in the system, the voltage drops, which causes cascading overload of the lines and transformers and accentuates the voltage decline [8].

2.2. Mitigation Techniques of Voltage Instability. Voltage stability analysis is useful in the design and selection of countermeasures to reduce voltage collapse and increase system stability. Solution to voltage instability can be grouped as system design and system operation measurements. Under system design measurement, voltage instability can be alleviated using reactive power compensation, coordination of protective devices, load shading, and design of voltage and reactive power using an Automatic Voltage Regulator (AVR). Also, system operation measurements can be operators' action and spinning reserve [9, 10]. Furthermore, the occurrence of voltage instability in the power system can also be controlled at the generator station, transmission, and distribution stations.

2.3. FACTS Devices. Flexible Alternative Current Transmission System (FACTS) stands for integrating power electronics equipment with the power system network [11]. The concept of FACTS refers to a family of power electronics-based devices able to enhance AC system controllability and stability and to increase power transfer capability. FACTS devices have several advantages, such as transmission capacity enhancement, power flow control, transient stability improvement, power oscillation damping, voltage stability, and control. The FACTS are classified as shunt, series, or a combination of series and shunt based on the connection to the system [12]. Table 1 shows some of the classifications and purposes of FACTS devices. STATCOM and SVC are the most adaptive shunt devices that are connected in shunt with the system. In the abnormal condition of the system, STATCOM is the most selective device to overcome the spread of abnormalities throughout the system. In this paper's work, the STATCOM device is selected as a compensator due to its more extensive and constant compensation current (independent of the system voltage), linear change of absorption

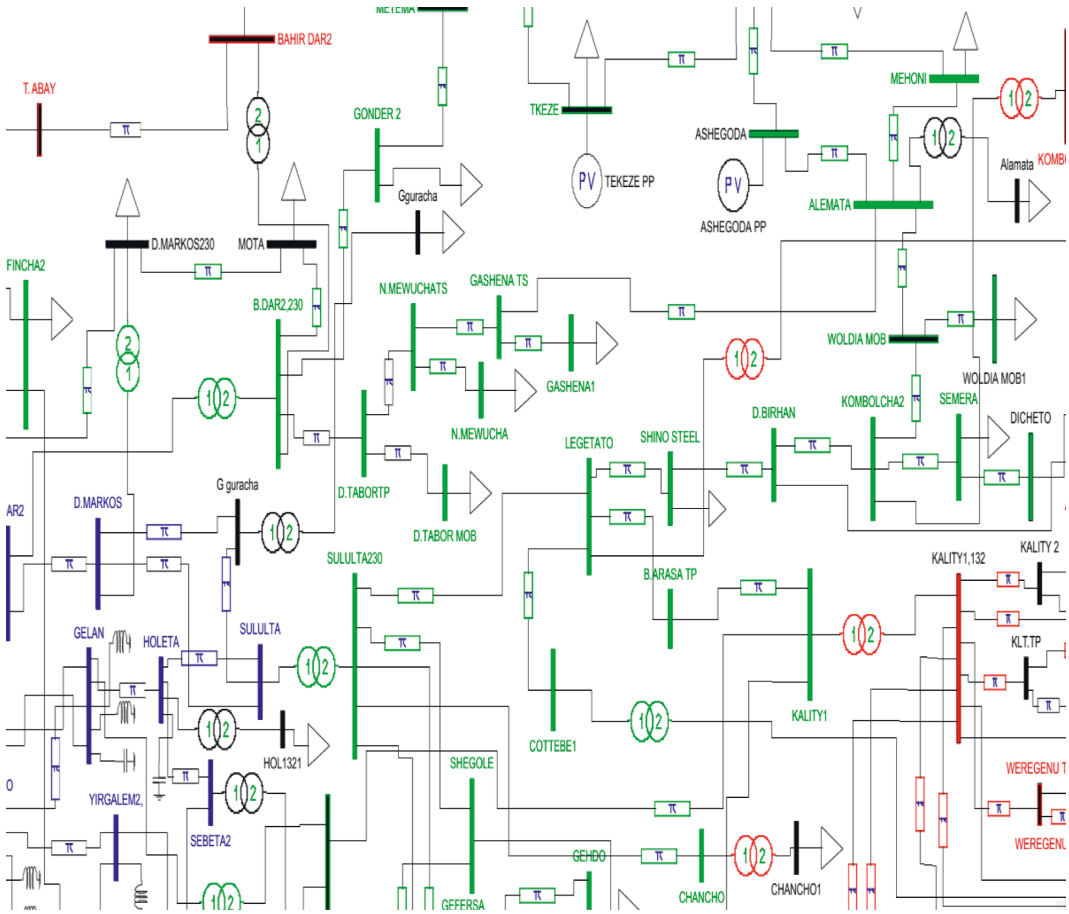

Figure 1: Modeling of Ethiopian Electric Power network.

and generation of reactive power, and fast action response [13].

The contribution of this paper includes the following points:

(i) Load flow analysis is performed to get the results of power system variables (voltage magnitude, phase angle, active power, reactive power, and power loss) and evaluate voltage stability indices and optimization functions using the results from the load flow.

(ii) A user-defined voltage stability index is formulated, which includes the effect of both active power and transmission line conductance on the voltage stability and compare the values of this index with other indices in terms of identifying the most voltage unstable buses by using load increasing tests.

(iii) The PSO algorithm is implemented to find the best location and size of STATCOM to enhance the voltage profile and minimize system power loss.

(iv) verifies the voltage unstable bus most identified by voltage stability indices and the best placement of STATCOM using PSO algorithm.

3. Proposed Method for Voltage Stability Analysis

3.1. Load Flow Analysis. Load flow studies are necessary for power system planning, economic operation, and expansion, as well as improving the existing systems, scheduling, and exchanging power between electric utilities. They are also important for other analyses, such as voltage stability analysis, transient stability analysis, contingency analysis, and state estimation. Therefore, load flow analysis is the basic power system computation tool to determine power system operation conditions. Active and reactive power injection of each bus, the phase angle and voltage magnitude of each bus, and the active and reactive power loss of each line represent the main information gained from the load flow analysis. Two of the four quantities, active power, reactive power, voltage magnitude, and phase angle, are specified for each bus, while the other two are calculated. The specified quantities are determined by the bus types. The Gauss-Seidel method, the Newton-Raphson method, and the Fast Decoupled Load Flow method are the most popular methods for conducting load flow analysis [14]. For large systems, the NR method is the most popular and selective because of its versatility, reliability, and accuracy.

Table 1: Classification of FACTS device.

Types of FACTS devices	Groups of the devices	Purposes/functions/
Shunt devices	STATCOM and SVC	Prove a specific bus's voltage profile, transient stability, and power oscillation damping
Series devices	TCSC, TSSC, and SSSC	Enhance the voltage stability limit, transient stability margin, power oscillation damping, and subsynchronous oscillation damping
Series and shunt devices	UPFC	Provide multifunctional flexibility required to solve many of the problems

3.2. Voltage Stability Indices (VSIs). Different methods have been proposed to compute static and dynamic voltage stability analysis to prevent and protect power systems from limit violence [15]. Continuation power flow, modal analysis, P-V curve, Q-V cure, and voltage stability indices are the most popular methods in voltage stability analysis. Additionally, load change cases and line and/or generator contingency cases are the usual system testing methods to analyze system security. In this paper, the load change test with the voltage stability index method is selected due to its capability to quantify the current operations of the system parameters. Therefore, some of the voltage stability indices that are used in this thesis work are explained below.

3.2.1. Fast Voltage Stability Indices. The fast voltage stability index (FVSI) was established by [16] using the same power transmission in two bus system concepts. This method needs more computation time and large storage, and it is more feasible for radial system network.

$$\mathrm{FVSI} = \frac{4 \times \mathrm{Z}^2 \mathrm{Q}_j}{\mathrm{V}_i^2 \mathrm{X}_{\mathrm{ij}}}. \tag{1}$$

3.2.2. Modified Voltage Stability Indices. The authors of [17] derived the modified voltage stability indices for the N-bus system. In this proposed method, the effect of transmission line conductance and active power, as well as the phase angle of the voltage, is neglected.

$$\mathrm{MVSI}_i = \frac{4\mathrm{Q}_i \times \mathrm{B}_{\mathrm{ii}}}{\left(\sum_{\substack{j=1 \\ j \neq i}}^{\mathrm{Nb}} \mathrm{V}_j \mathrm{B}_{\mathrm{ij}} \right)^2}. \tag{2}$$

3.2.3. Advanced Voltage Stability Indices. This method is a user-defined method voltage stability index that is derived from the load flow equation for an N-bus system by considering the effects of active power and transmission line conductance on the voltage stability of the given bus while ignoring the voltage phase angle. The equation is derived from the large network model shown in Figure 2.

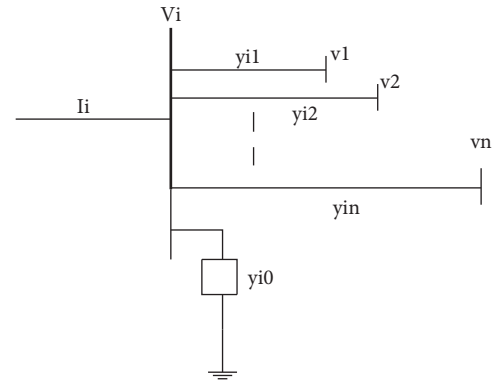

Figure 2: N-bus network model.

$$S_i = P_i + \mathrm{jQ}_i = V_i \times I_i^*. \tag{3}$$

$$I_i^* = \frac{P_i + \mathrm{jQ}_i}{V_i}. \tag{4}$$

From the formation of bus loading equation, the current injection into load bus i is derived by using Kirchhoff's current law (KCL).

$$I_i = V_i Y_{\mathrm{ii}} + \sum_{\substack{j=1 \\ j \neq i}}^{\mathrm{Nb}} V_j Y_{\mathrm{ij}} I_i^* = \left(V_i Y_{\mathrm{ii}} + \sum_{\substack{j=1 \\ j \neq i}}^{\mathrm{Nb}} V_j Y_{\mathrm{ij}} \right)^*. \tag{5}$$

$$I_i^* = V_i \angle - d_i \left[G_{\mathrm{ii}} - \mathrm{jB}_{\mathrm{ii}} \right] + \sum_{\substack{j=1 \\ j \neq i}}^{\mathrm{Nb}} V_j \angle - d_j \left[\mathrm{G}_{\mathrm{ij}} - \mathrm{jB}_{\mathrm{ij}} \right]. \tag{6}$$

By equating, we have

$$\frac{P_i + jQ_i}{V_i} = V_i \angle - d_i \left[G_{\mathrm{ii}} - \mathrm{jB}_{\mathrm{ii}} \right] + \sum_{\substack{j=1 \\ j \neq i}}^{\mathrm{Nb}} V_j \angle - d_j \left[\mathrm{G}_{\mathrm{ij}} - \mathrm{jB}_{\mathrm{ij}} \right]. \tag{7}$$

By rearranging and collecting like terms, the power equation at load bus i becomes

$$P_i = V_i^2 G_{ii} + \sum_{\substack{j=1 \\ j \neq i}}^{Nb} V_i V_j \left[G_{ij} \cos\left(\delta_i - \delta_j\right) + B_{ij} sin\left(\delta_i - \delta_j\right) \right]$$
$$Q_i = -V_i^2 B_{ii} + \sum_{\substack{j=1 \\ j \neq i}}^{Nb} V_i V_j \left[G_{ij} sin\left(\delta_i - \delta_j\right) - B_{ij} cos\left(\delta_i - \delta_j\right) \right]. \quad (8)$$

Since the magnitude of angle difference between sending end and receiving end is small and $\delta_i - \delta_j$ approaches zero, the power equation becomes

$$P_i = V_i^2 G_{ii} + \sum_{\substack{j=1 \\ j \neq i}}^{Nb} V_i V_j G_{ij} Q_i = -V_i^2 B_{ii} - \sum_{j=1}^{Nb} B_{ij} V_i V_j \quad (9)$$

Now adding the above two equations,

$$P_i + Q_i = V_i^2 \left[G_{ii} - B_{ii} \right] + V_i \left(\sum_{\substack{j=1 \\ j \neq i}}^{Nb} V_j \left[G_{ij} - B_{ij} \right] \right). \quad (10)$$

Now, the equation becomes quadratic and the roots are solved with respect to V_i.

$$V_i^2 \left[G_{ii} - B_{ii} \right] + V_i \left(\sum_{\substack{j=1 \\ j \neq i}}^{Nb} V_j \left[G_{ij} - B_{ij} \right] \right) - \left(P_i + Q_i \right) = 0$$
$$V_{i(1,2)} = \frac{-\left(\sum_{\substack{j=1 \\ j \neq i}}^{Nb} V_j \left[G_{ij} - B_{ij} \right] \right) \pm \sqrt{\left(\sum_{\substack{j=1 \\ j \neq i}}^{Nb} V_j \left[G_{ij} - B_{ij} \right] \right)^2 + 4 \left[G_{ii} - B_{ii} \right] \left(P_i + Q_i \right)}}{2 \left[G_{ii} - B_{ii} \right]}. \quad (11)$$

Now, to have real and stable voltage at load bus i, the discriminant should be greater than or equal to zero. Thus,

$$\left(\sum_{\substack{j=1 \\ j \neq i}}^{Nb} V_j \left[G_{ij} - B_{ij} \right] \right)^2 + 4 \left[G_{ii} - B_{ii} \right] \left(P_i + Q_i \right) \geq 0$$

$$AVSI = \frac{-4 \left(G_{ii} - B_{ii} \right) \left(P_i + Q_i \right)}{\left(\sum_{\substack{j=1 \\ j \neq i}}^{Nb} V_j \left[G_{ij} - B_{ij} \right] \right)^2} \leq 1 \quad (12)$$

$$AVSI = \frac{-4 \left(G_{ii} - B_{ii} \right) \left(P_i + Q_i \right)}{\left(\sum_{\substack{j=1 \\ j \neq i}}^{Nb} V_j \left[G_{ij} - B_{ij} \right] \right)^2}$$

The flow chart of VSIs with load change test to determine the weakest bus is shown in Figure 3.

All the indices including the user-defined voltage stability index are used to identify the stability region or the closeness of a given bus to the voltage collapse point by increasing and decreasing loads. The values of VSIs are displayed for each bus. Thus, if the values of VSIs of a given bus are greater than 1.00, the bus is a weak bus, whereas the bus is stable if the values of VSIs are less than 1.00. Therefore, if the value of the VSI of a given bus approaches 1.00, the bus approaches the collapse point.

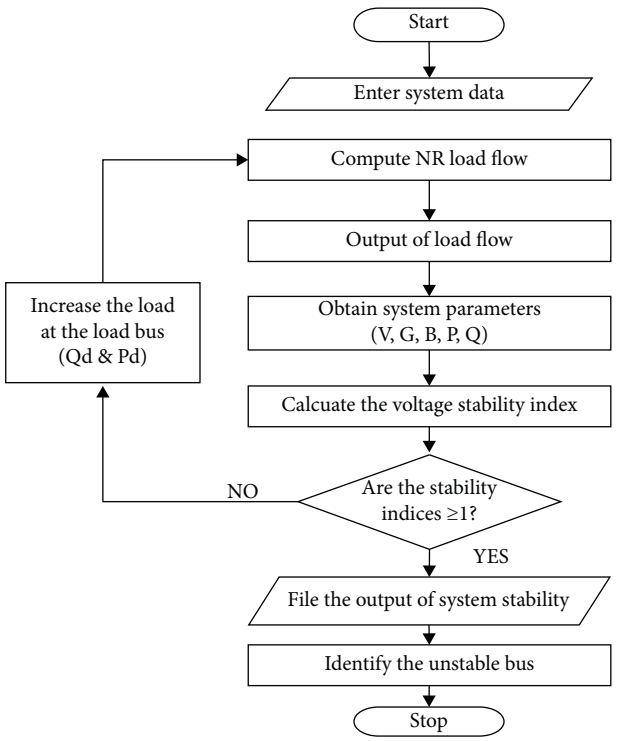

Figure 3: Flow charts of voltage stability indices.

3.3. Optimal Location of STATCOM. Because results vary depending on network topology, configurations, and contingencies such as load increment or variation, generator, or line tripping, the candidate or weakest buses identified by voltage stability indices may not lead to optimal solutions. These drawbacks can be overcome using metaheuristic optimization techniques, in which algorithms assist in determining the best location, number, and size of STATCOMs based on the objectives used and constraints.

Different optimization techniques have been proposed to find the optimal size and location of reactive power compensation devices. Among them, conventional methods (such as linear programming, nonlinear programming, and sequential quadratic programming) and metaheuristic methods are usual optimization methods [18]. Thus, swarm intelligent algorithms are subbranches of metaheuristics bioinspired based algorithms and are categorized by different methods. Under swarm intelligent algorithms, the particle swarm optimization algorithm is one of the popular methods to find the optimal size and placement of reactive power compensation devices.

Particle swarm optimization (PSO) is a family of swarm intelligent algorithms derived from the social behavior of animals such as birds and fish schools, bees, termites, and ants [19]. In this paper, the particle swarm optimization (PSO) technique is used as an optimization method due to it being more flexible and robust than conventional methods and being more suitable for searching complicated and uncertain areas. It is also easy to implement, with small computational burden and fast convergence. The two following formulas are basic for the PSO algorithm:

$$V_i^{j+1} = w \times V_i^j + c_1 r_1\left(P_{\text{best}(i)}^j - X_i^j\right) + c_2 r_2\left(G_{\text{best}(i)}^j - \mathrm{X}_i^j\right),$$
$$X_i^{j+1} = X_i^j + V_i^{j+1}, \tag{13}$$

where

(i) V_i^{j+1} is the velocity of i^{th} particle and j^{th} iteration.

(ii) X_i^{j+1} is the position of i^{th} particle and j^{th} iteration.

(iii) c_1 and c_2 are the weighting coefficients.

(iv) $\mathrm{P}_{\text{best}(i)}^j$ is the best of individual functional values of each i^{th} particle and j^{th} iteration by comparing the current iteration and the previous iteration.

(v) $\mathrm{G}_{\text{best}(i)}^j$ is the global best of functional values of each i^{th} particle and j^{th} iteration by comparing the current iteration and previous iteration.

(vi) r_1 and r_2 are random values between 0 and 1.

(vii) w is the inertia weight, which can be determined by

$$\mathrm{w} = \mathrm{w}_{\text{maxi}} - \left(\frac{\mathrm{w}_{\text{maxi}} - \mathrm{w}_{\text{mini}}}{i_{\text{maxi}}}\right) \times i_{\text{current}}. \tag{14}$$

3.3.1. Formation of Objective Functions. In this paper, two minimization objective functions are carried out to find the optimal size and location of STATCOM to improve the voltage profile and minimize power loss. Thus, active power loss and the voltage deviation index are the two objective functions.

$$\mathrm{MinF}_1 = \sum_{\mathrm{b=nb}}^{\mathrm{Nline}} \mathrm{G}_{i,j}\left(2\mathrm{V}_i \times \mathrm{V}_j \cos\left(\delta_{\mathrm{ij}}\right) - \mathrm{V}_i^2 + \mathrm{V}_j^2\right),$$
$$\mathrm{MinF}_2 = \mathrm{MinF}_2 = \sum_{i=1}^{\mathrm{nlb}} \left(1 - \mathrm{V}_i\right)^2, \tag{15}$$

3.3.2. Equality Constraints. From the power balance equation,

$$\mathrm{Pg}_i - \mathrm{Pd}_i - \sum_{j=1}^{\mathrm{Nb}} \mathrm{V}_i \mathrm{V}_j\left(\mathrm{G}_{\mathrm{ij}} \cos\ \delta_{\mathrm{ij}} + \mathrm{B}_{\mathrm{ij}} \sin\ \delta_{\mathrm{ij}}\right) = 0,$$
$$\mathrm{Qg}_i - \mathrm{Qd}_i - \sum_{j=1}^{\mathrm{Nb}} \mathrm{V}_i \mathrm{V}_j\left(\mathrm{G}_{\mathrm{ij}} \sin\ \delta_{\mathrm{ij}} + \mathrm{B}_{\mathrm{ij}} \cos\ \delta_{\mathrm{ij}}\right) = 0. \tag{16}$$

3.3.3. Inequality Constraints. The voltage magnitude limit of all buses is as follows:

$$V_i^{\min} \le V_i \le V_i^{\max} i \in \mathrm{Nb}. \tag{17}$$

The generation reactive power limits at all generator buses are as follows:

$$\mathrm{Qg}_i^{\min} \le \mathrm{Qg}_i \le \mathrm{Qg}_i^{\max} i \in \mathrm{Ngb}. \tag{18}$$

(1) Define control variables with allowable ranges and appropriate PSO parameter values, as well as input data for the transmission lines and buses.
(2) Take iter = 0
(3) Generate the population of particles and their velocities randomly.
(4) Run NR load flow for each particle to calculate power losses and voltage performance index.
(5) Compute the objective function of each particle using equation (23).
(6) Calculate the personal best (Pbest) of all particles and the global best (Gbest) of all particles from their objective function.
(7) Iter = iter + 1
(8) Compute the velocity of each particle using equation (19) and adjust it if its limit gets violated.
(9) Update the position of each particle using equation (20).
(10) Compute the objective function of each particle using equation (23).
(11) For each particle, if the personal best of current fitness (P) is better than the P best of previous fitness, then P best = P.
(12) Set Pbest and Gbest to their best.
(13) Go to step number 7, until the maximum number of iterations is completed.
(14) Gbest particle coordinates give optimized values of control variables and their fitness gives minimized values of power losses and voltage magnitude within the standard limit.

Algorithms

The values of voltage stability index (VSI) should be between 0 and 1.

$$0 \leq \mathrm{VSI}_i < 1. \tag{19}$$

The constraints of power flow limits of each transmission line are as follows:

$$\mathrm{S_l} \leq \mathrm{S}_l^{\max}. \tag{20}$$

The weighting factor is used to change multiobjective functions to single-objective functions. Therefore, from equations (13) and (14),

$$\begin{aligned} \mathrm{MinF} &= w_1 F_1 + w_2 F_2, \\ w_1 + w_2 &= 1. \end{aligned} \tag{21}$$

A static square penalty function is used to handle inequality constraints. So, the augmented objective function (fitness function) would be

$$\begin{aligned} &\text{objective function (fitness function)} \\ &\quad = \mathrm{MinF} + \text{penalty function}, \\ &\text{penalty function} = d_1 f\left(\mathrm{Qg}_i\right) + d_2 f\left(V_i\right) + \mathrm{d_3 f}\left(\mathrm{VSI}_i\right) \\ &\quad + \mathrm{d}_4 f\left(\mathrm{S_l}\right), \end{aligned} \tag{22}$$

where d_1, d_2, d_3, d_4 are penalty factors

$$\begin{aligned} &\text{objective function (fitness function)} \\ &= \mathrm{w_1 F_1} + \mathrm{w_2 F_2} + \text{penalty functions}. \end{aligned} \tag{23}$$

The system convergence is reached when the difference between the current and previous iterations' functional value becomes very small or the computation reaches the maximum iteration. Figure 4 shows the flow chart of PSO algorithm.

4. Results and Discussion

In the base case, nine buses are detected as unstable, as shown in Table 2. Even if the voltage magnitude of some buses corresponding to the current operating load is within the limit, the bus voltage stability indices of these buses are closed and beyond the unity value. This means that the voltage stability of the given bus not only depends on the voltage violation limit but also depends on the current operating points, the reactive power supply, the system network impedance, and configurations. Therefore, this indicates that the current operating point of these buses is approaching the maximum loading capacity. The range between the current operating point and the collapse point of these buses is small. Additionally, as shown in Table 2, the values of AVSI are higher than the values of the other two indices, which indicates that AVSI is more feasible to identify voltage unstable buses quickly. However, in Table 2, the values of FVSI for each bus are less than others, even if the bus is unstable. This indicates that this index is not feasible to identify the weakest buses for mushed and high-power systems. Rather, it is used for radial and distribution power systems. Therefore, active power and transmission conductance have an effect on the stability of bus voltage, and they cannot be neglected to study voltage stability assessments in high-voltage mushed systems. As shown in Table 2, bus number 162 is a more unstable bus as compared with the other buses.

The magnitude of voltage stability indices at the base case level is shown in Figure 5. Thus, the indices values of these buses are above unity and considered as unstable buses.

Even if some buses are voltage unstable based on the values of VSI in the base case, load increment techniques are also used to know the carrying capacity of the remaining stable buses and how much additional load they can take from the current operating point to their optimum operating limits. This helps with system isolation, maintenance, and power continuity. Therefore, as the load increases 10% from the base case, the voltage stability indices also increase more and the voltage magnitude of the buses decreases. Due to decreasing the voltage magnitude, the voltage deviation index (VDI) increases as shown in Figure 6.

When the load is increased by 20% and 30% from the base case, the bus voltage magnitude is decreased too, and

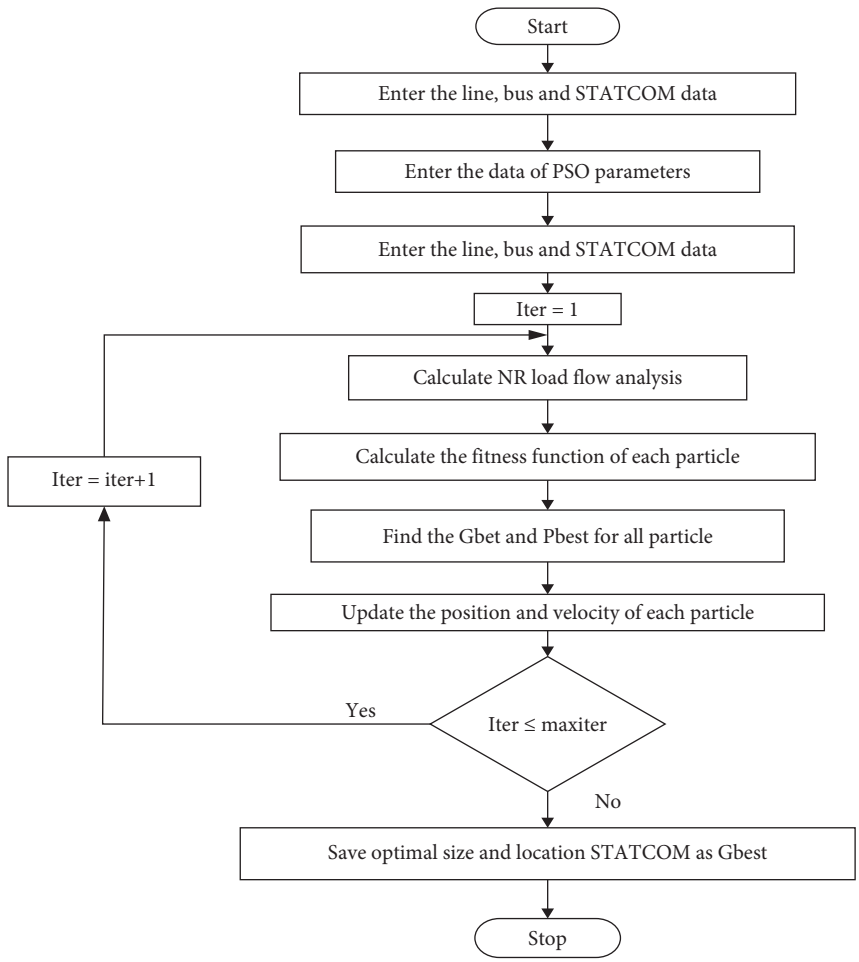

Figure 4: Flow chart of PSO algorithm.

Table 2: Values of stability indices at base case and 10% load increasing conditions.

Bus no.	Base case				Bus no.	10% loading condition				Rank
	MVSI	AVSI	FVSI	VDI		MVSI	AVSI	FVSI	VDI	
6	0.1407	0.6154	0.0235	0.069	6	0.1564	0.6408	0.0359	0.06	9
19	0.8581	1.4275	0.0059	0.0018	19	0.9506	1.4844	0.0067	0.0055	5
27	0.6305	1.2553	0.0070	0.0349	27	0.7024	1.3097	0.0078	0.0235	6
35	0.3394	0.7210	0.0259	0.0303	35	0.3777	0.7521	0.0288	0.0261	8
108	0.4171	1.1747	0.0235	0.0012	108	0.4648	1.2091	0.0067	0.0015	7
162	8.2253	14.2333	0.0060	0.0276	162	9.2340	15.0947	0.0884	0.031	1
202	1.7202	8.1578	0.0792	0.0463	202	1.9071	8.4844	0.1491	0.05	2
207	1.3101	2.7866	0.1341	0.0069	207	1.4463	2.8792	0.1465	0.0008	4
209	1.5376	7.5133	0.1331	0.0489	209	1.7060	7.8248	0.0610	0.053	3

the voltage stability indices are increased. As shown in Table 3, the voltage magnitude of most buses has decreased significantly, whereas the voltage deviation index has increased. In Table 3, seven buses are outside the stability regions, and three buses are close to the critical point.

Figure 7 shows the comparison of voltage stability indices as the load increases to 20% of the base case. As shown in Figure 7, the advanced voltage stability index is more feasible than the fast voltage stability index and the modified voltage stability index to determine the most voltage unstable buses. This indicates that the transmission line conductance as well as active power load has an effect on the voltage stability and it cannot be neglected on the formation of indices.

When the load is further increased to 30%, additional buses approach the instability region. As shown in Figure 8, the value of the voltage stability indices also increases as the

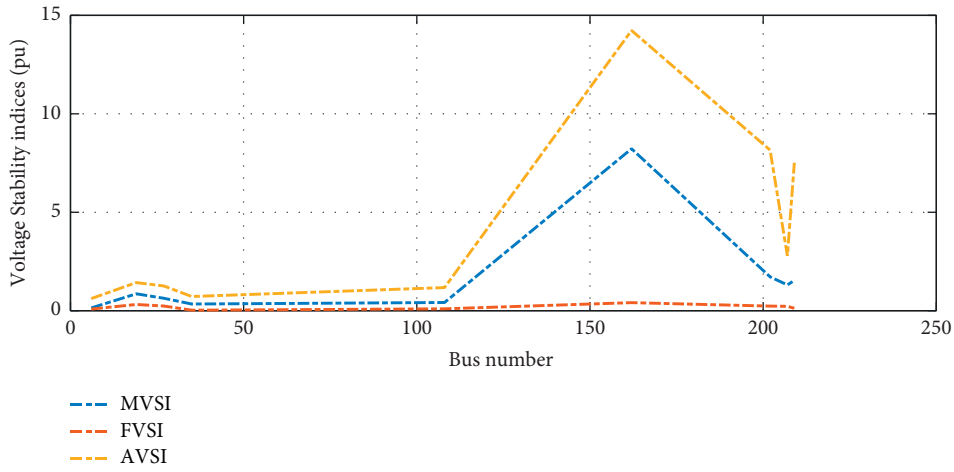

Figure 5: Voltage stability indices at base case.

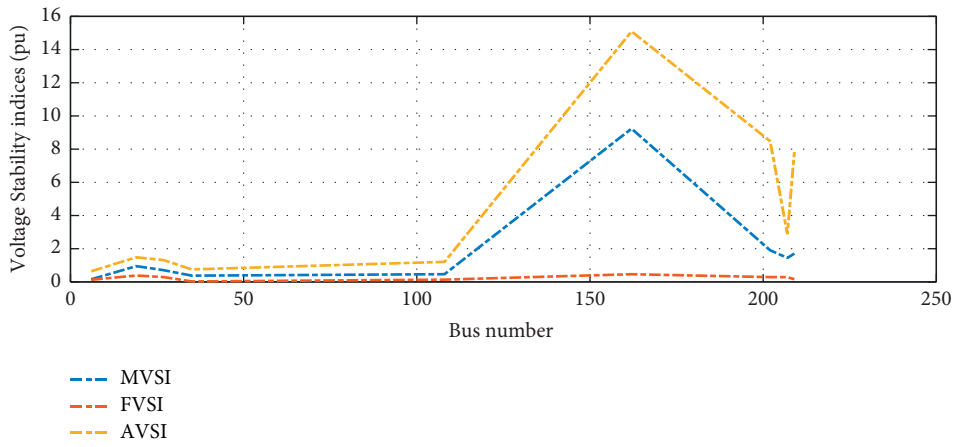

Figure 6: Voltage stability indices at 10% load increase.

Table 3: Values of stability indices at 20% and 30% load increasing conditions.

Bus no.	20% loading				Bus no.	30% loading				Rank
	MVSI	AVSI	FVSI	VDI		MVSI	AVSI	FVSI	VDI	
6	0.1725	0.6667	0.0397	0.068	6	0.1888	0.6981	0.0435	0.0229	10
19	1.0443	1.5421	0.0076	0.0092	19	1.1394	1.6006	0.0085	0.0129	5
27	0.7761	1.3653	0.0086	0.0121	27	0.8516	1.4224	0.0094	0.0007	6
35	0.4169	0.7801	0.0318	0.0219	35	0.54569	0.8107	0.0348	0.0177	9
108	0.5404	1.2440	0.0072	0.0019	108	0.5529	1.2794	0.0078	0.0023	7
162	10.2834	15.8954	0.0979	0.0344	162	11.3754	16.7280	0.1077	0.0886	1
194	0.2254	0.7871	0.0548	0.0046	194	0.2477	0.8229	0.0549	0.0056	8
202	2.0966	8.8160	0.1646	0.0536	202	2.2891	9.1527	0.1804	0.0573	2
207	1.5922	2.9726	0.1598	0.0084	207	1.7216	3.0666	0.1732	0.0161	4
209	1.8772	8.1416	0.0673	0.0571	209	2.0515	8.4638	0.0781	0.0612	3

load increases. Moreover, the loading capacity is more stressed as you increase the load.

The voltage magnitude for Ethiopian Electric Power (EEP) of each bus before STATCOM connected to the bus is shown in Figure 9. Based on the result, the voltage magnitude of some buses is below and above the limit (0.95 and 1.05).

Based on the result, after STATCOM is connected at bus number 6, the voltage magnitude of all buses is within the range. Also, based on the draft grid code of Ethiopian electric power operations, the maximum and minimum ranges of voltage magnitude are 1.05 and 0.95, respectively, and the result has been met within that range, as shown in Figure 10.

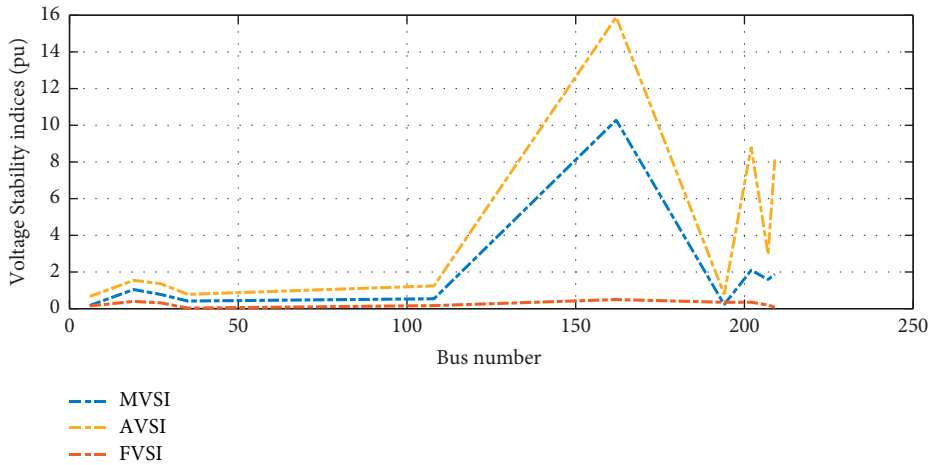

Figure 7: Voltage stability indices at 20% load increase.

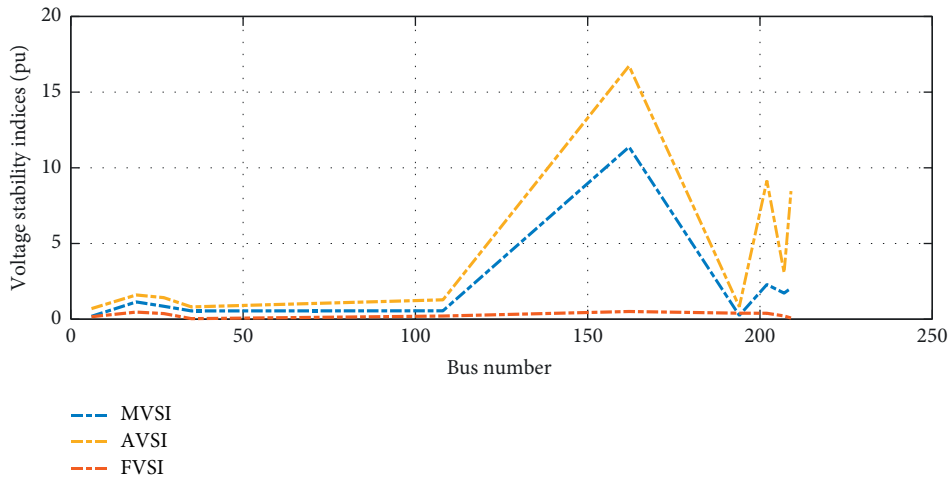

Figure 8: Voltage stability indices at 30% load increase.

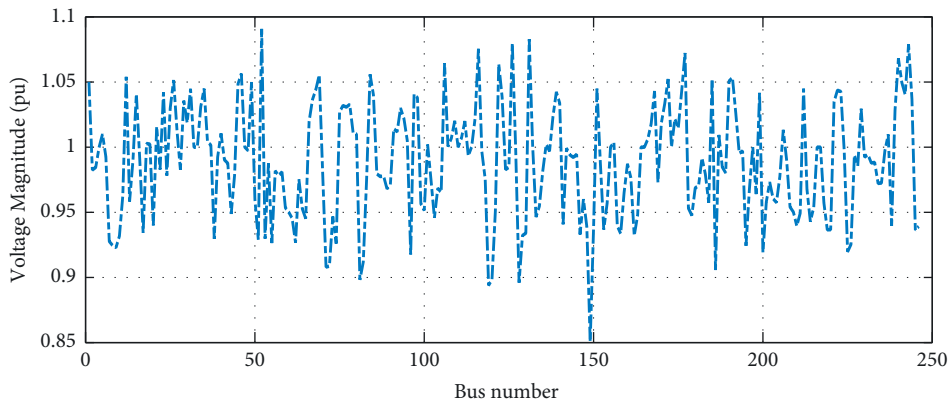

Figure 9: Voltage magnitude before STATCOM is connected.

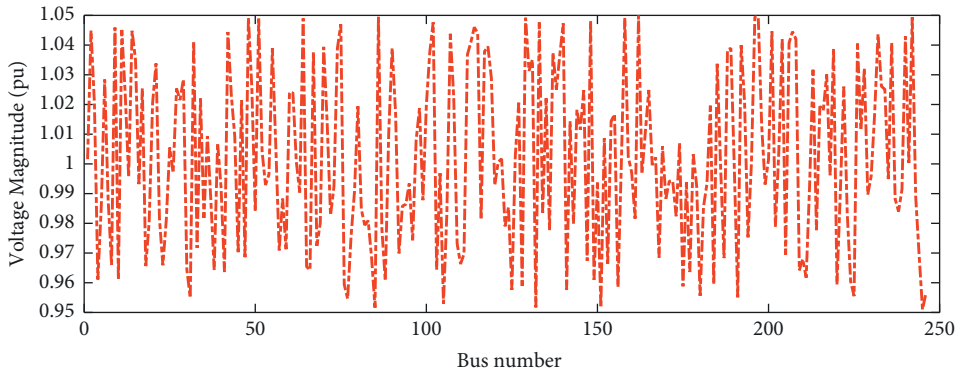

Figure 10: Voltage magnitude after STATCOM is connected.

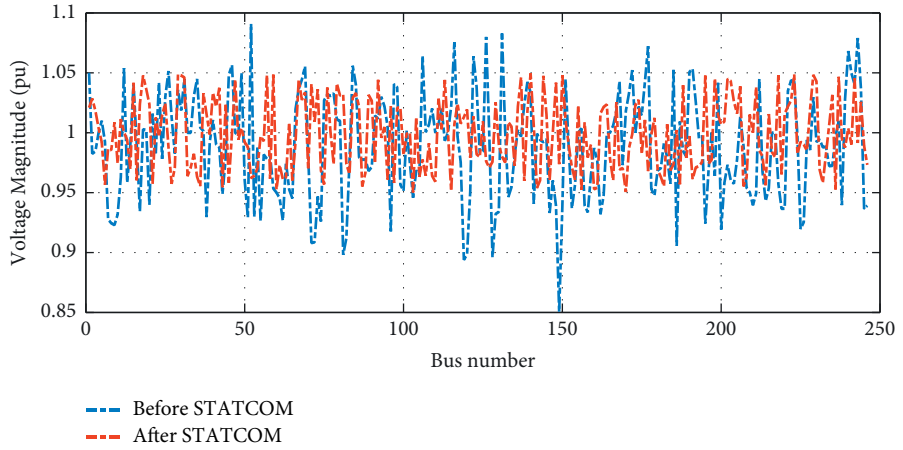

Figure 11: Comparison of voltage magnitude before and after STATCOM is connected.

When comparing the voltage magnitude before and after STATCOM is connected to the system, the voltage magnitude of all buses is improved, and it obeys both Ethiopian draft grid code and IEEE standard voltage limits as shown in Figure 11.

5. Conclusion

This thesis aimed to improve the voltage profile and minimize power loss for Ethiopian Electric Power (EEP) systems, including 400 kV, 230 kV, and 132 kV transmission systems. The system has been modeled with PSAT (Power System Analysis Toolbox) and the power flow analysis has been performed using the Newton-Raphson method in MATLAB code. Besides, particle swarm optimization (PSO) methods with two objective functions and five constraints have been used to find the optimal location and size of the STACOM. Also, a user-defined advanced voltage stability index (AVSI) has been adopted to identify unstable buses, which is more feasible for meshed and high-voltage transmissions. The most voltage unstable bus identified by voltage stability indices is bus 162, whereas the optimal placement is bus 6. This notifies us that the weakest bus may not be the optimal placement of compensator devices. Therefore, STACOM was placed at bus number 6, and the voltage magnitude had improved. After connecting to 46MVAR, connected at bus number 6, the voltage magnitude had improved and the power loss had decreased from 46.65 MW to 33.32 MW.

6. Future Work

In this paper, the voltage stability was studied based on the load increments on each bus at the same increasing rate at a time. The next researchers can do this by increasing the load of each bus at different times and scales. This will help to study the effect of each load on the system's stability and will also help to determine the behavior of each load.

Data Availability

The data used to support the findings of this study are available from the corresponding author upon request.

Conflicts of Interest

The authors declare that they have no conflicts of interest.

Supplementary Materials

(i) Voltage magnitude with and without connected STATCOM. (*Supplementary Materials*)

References

[1] O. Mogaka, R. Orenge, and J. Ndirangu, "Static voltage stability assessment of the Kenyan power network," *J. Electr. Comput. Eng.*, vol. 2021, p. 2021.

[2] B. B. Adetokun and C. M. Muriithi, "Application and control of flexible alternating current transmission system devices for voltage stability enhancement of renewable-integrated power grid: a comprehensive review," *Heliyon*, vol. 7, no. 3, Article ID e06461, 2021.

[3] E. C. Newjec, *Inc, Japan International Cooperation, "Federal Democratic Republic of Ethiopia Ethiopian Electric Power STUDY on ENVIRONMENTAL and SOCIAL CONSIDERATIONS for ADDIS ABABA PROJECT IN the FEDERAL DEMOCRATIC REPUBLIC of ETHIOPIA*, October, 2018.

[4] M. Okelola, S. O. Ayanlade, and E. I. Ogunwole, "Particle swarm optimization for optimal allocation of STATCOM on transmission network particle swarm optimization for optimal allocation of STATCOM on transmission network," *Conf. Ser.*, p. 2021, 1880.

[5] R. T. Singh Rawat Mahiraj, "Optimal placement of TCSC and STATCOM for voltage stability enhancement in transmission network," in *Proceedings of the 2018 5th IEEE Uttar Pradesh Sect. Int. Conf. Electr. Electron. Comput. Eng*, pp. 1–6, Gorakhpur, India, November2018.

[6] M. G. Yenealem, L. M. H. Ngoo, D. Shiferaw, and P. Hinga, "Management of voltage profile and power loss minimization in a grid-connected microgrid system using fuzzy-based STATCOM controller," *Journal of Electrical and Computer Engineering*, p. 1, 2020.

[7] S. Bhongade and A. Tomar, "Optimal reactive power dispatch optimization using STATCOM," *Journal of the Institution of Engineers: Serie Bibliographique*, vol. 102, no. 2, pp. 277–293, 2021.

[8] P. Pourbeik, P. S. Kundur, and C. W. Taylor, "The anatomy of a power grid blackout - root causes and dynamics of recent major blackouts," *IEEE Power and Energy Magazine*, vol. 4, no. 5, pp. 22–29, 2006.

[9] S. Issue, I. Journal, and C. Proceedings, "Voltage collapse : causes and prevention," vol. 4, no. 02, pp. 2–5, 2016.

[10] P. Kundur, *Power System Stability and Control*, McGraw-Hill, NeyYork San Francisco Washington , D.c, 2007.

[11] H. L. Ferreira, A. L'Abbate, G. Fulli, and U. Häger, "Flexible alternating current transmission systems (FACTS) devices," *Power Systems*, vol. 69, pp. 119–156, 2013.

[12] A. Al Ahmad and R. Sirjani, "Optimal Placement and Sizing of Multi-type FACTS Devices in Power Systems Using Metaheuristic Optimisation Techniques: An Updated Review," *Ain Shams Eng. J.*vol. 11, no. 3, 2019.

[13] A. S. Siddiqui and T. Deb, "Voltage Stability Improvement Using STATCOM and SVC," *International Journal of Computer Applications*, vol. 88, pp. 42–47, August 2016.

[14] H. K. Ahmad, "Ac Power Flow Analysis Using Fast Decoupled Newton-Raphson Algorithm Compared with Gaussian- Seidel Approach," *JOURNAL OF OPTOELECTRONICS LASER*, vol. 41, no. 3, March, 2022.

[15] H. Zaheb, M. S. S. Danish, T. Senjyu et al., "A contemporary novel classification of voltage stability indices," *Applied Sciences*, vol. 10, no. 5, pp. 1–15, 2020.

[16] I. Musirin, T. K. A. Rahman', Novel Fast Voltage Stability Index (FVSI) for Voltage Stability Analysis in Power Transmission System," in *Proceedings of the*, pp. 265–268, 2002, Student Conference on Research and Developmenthttps://ieeexplore.ieee.org/xpl/conhome/8033/proceeding.

[17] T. G. Tella, S. S. Sitati, and G. N. Nvakoe, "Voltage Stability Assessment on Ethiopian 230 KV Transmission Network Using Modified Voltage Stability Indices," in *Proceedings of the 2018 IEEE PES/IAS PowerAfrica*, pp. 79–83, Cape Town, South Africa, June2018.

[18] Y. Muhammad, R. Khan, M. A. Z. Raja, F. Ullah, N. I. Chaudhary, and Y. He, "Solution of optimal reactive power dispatch with FACTS devices: a survey," *Energy Reports*, vol. 6, pp. 2211–2229, 2020.

[19] B. Ismail, N. I. Abdul Wahab, M. L. Othman, M. A. M. Radzi, K. Naidu Vijyakumar, and M. N. Mat Naain, "A comprehensive review on optimal location and sizing of reactive power compensation using hybrid-based approaches for power loss reduction, voltage stability improvement, voltage profile enhancement and loadability enhancement," *IEEE Access*, vol. 8, pp. 222733–222765, 2020.